VALENCE STATE PARTITIONING OF CR AND V BETWEEN OLIVINE-MELT AND PYROXENE-MELT IN EXPERIMENTAL BASALTS OF A EUCRITIC COMPOSITION. J.M. Karner[1] (jmk207@case.edu), J.H. Jones[2], and L. Le[3]. [1]Dept. of Earth, Environmental, and Planetary Sciences, Case Western Reserve University, Cleveland, OH. [2]Astromaterials Research Office, NASA Johnson Space Center, Houston, TX. [3]Jacobs, NASA Johnson Space Center, Houston, TX 77058.

Introduction: The partitioning of multivalent elements in basaltic systems can elucidate the oxygen fugacity (fO_2) conditions under which basalts formed on planetary bodies (Earth, Moon, Mars, asteroids). Chromium and V are minor and trace elements in basaltic melts, partition into several minerals that crystallize from basaltic melts, exist in multiple valence states at differing fO_2 conditions, and can therefore be used as oxybarometers for basaltic melts. Chromium is mostly 3+ in terrestrial basaltic melts at relatively high fO_2 values ($\geq$ IW+3.5), and mostly 2+ in melts at low fO_2 values ($\leq$ IW-1), such as those on the Moon and some asteroids [1]. At intermediate *f*O2s, (i.e., IW-1 to IW+3.5), basaltic melts contain both Cr^{3+} and Cr^{2+}. Vanadium in basaltic melts is mostly 4+ at high fO_2, mostly 3+ at low fO_2, and a mix of V^{3+} and V^{4+} at intermediate fO_2 conditions. Understanding the partitioning of Cr and V into silicate phases with changing fO_2 is therefore critical to the employment of Cr and V oxybarometers.

In this abstract we examine the equilibrium partitioning of Cr and V between olivine/melt and pyroxene/melt in experimental charges of a eucritic composition produced at differing fO_2 conditions. This study will add to the experimental data on *D*Cr and *D*V (i.e., olivine/melt, pyroxene/melt) at differing fO_2, and in turn these *D* values will be used to assess the fO_2 of eucrite basalts and perhaps other compositionally similar planetary basalts.

Samples and analytical techniques: The samples used in this study are experimental crystallization products from the Sioux County eucrite composition doped with 1000 ppm V and Sc [2]. The charges were produced at fO_2 values of IW-1, IW, IW+2 and include both isothermal and cooling runs. Isothermal charges were produced by first homogenizing the mix at temperatures above the liquidus (~1195 °C), air-quenched then put it back to the desired temperature and holding for 24 to 48 hours. Cooling charges were made by first homogenizing above the liquidus, air-quenched then put it back to just below the liquidus at 1190 °C, (although our first attempts cooled from 1160 °C), and subsequently cooling to the desired temperature at a rate of 1 °C/hr or 0.2 °C/hr.

Major and minor element compositions of olivine, pyroxene and melt were determined using a Cameca SX100 electron microprobe. WDS was performed using a voltage of 15 kV, beam current of 20 nA, and beam size of ~3 μm for minerals and melt. Counting times were 20s for major and minor elements and 120s for V and Sc. Natural minerals including forsterite, chromite, and amphibole were used as standards, while V and Sc were calibrated on the respective metals of each. Olivine, pyroxene, and melt analyses were critically evaluated as to proper wt.% oxide totals, stoichiometry, and charge balance based on ideal mineral formulas. *D*Cr, *D*V, and *D*Sc values were determined by measuring several pairs of mineral rims and adjacent glass and then taking the average.

Results: Figure 1 shows a typical experimental charge containing subhedral olivine grains (bright gray) and skeletal, "soda straw" pyroxenes (dark gray) in a matrix of melt (glass). In general, the charges shared a common silicate crystallization sequence of olivine crystallization around 1190 °C, followed by olivine + pyroxene at ~1180, and no change down to a temperature of at least 1130 °C. Plagioclase was only found in two charges, both produced at IW-1 and both cooling experiments. The first crystallized olivine, pyroxene and plagioclase when cooled from 1190 to 1150 °C at 1 °C/hr and the second crystallized pyroxene and plagioclase when cooled from 1160 to 1100 °C at 1 °C/hr.

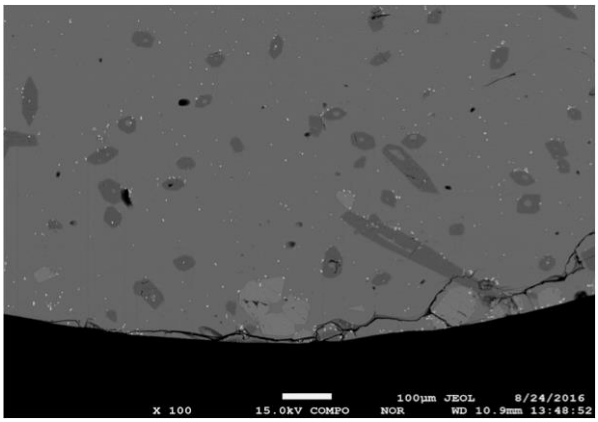

Figure 1. BSE image of charge S12, produced isothermally at IW and 1163 °C.

Discussion: Our silicate crystallization sequences differ from those found by Stolper [3], when he performed isothermal melting experiments on the natural Sioux County meteorite. Stolper found olivine crystallizing first (1195 °C), followed closely by pyroxene at 1180 and then plagioclase at 1170; olivine was not present in runs below 1165 °C. So, our experiments differ

from [3] in temperature of phase appearances, but also in the existence of olivine at low temperatures; we expected it to react with melt to form pyroxene [3]. We are presently performing more experiments and tweaking variables such as homogenization temperature and time, cooling start temperature and cooling rate in order to address these issues. However, we have evaluated the current experiments and some useful partitioning information is presented here.

Table 1 presents Cr, Sc, and V wt. % oxide concentrations in olivine and melt for each charge. These experiments all show homogenous olivine grains with olivine/melt K*D* FeO/MgO ≈ 0.35, which suggests the grains are approaching equilibrium with the melt for this iron-rich eucrite bulk composition [4]. *D*Cr olivine/melt is about unity at IW-1, IW, and IW, even though the Cr^{2+}/Cr^{3+} ratio is decreasing with increasing fO_2. The reason for this is that DCr^{2+} and DCr^{3+} olivine/melt are about equal; Cr^{2+} substition into the olivine structure for Mg^{2+} or Fe^{2+} causes no charge balance problems but it is just a little big for the M1 site in olivine, while Cr^{3+} fits nicely into the olivine M1 site but requires charge balance [1]. These results are almost identical to those measured by [3] and are consistent with the predictions by [5].

Our *D*Sc olivine/melt values (Table 1) are not consistent at all, which is most likely a consequence of attempting to measure low concentrations of Sc in melt (i.e., near detection levels), which in turn can lead to erroneous *D*Sc values. A linear equation by [6] relating *D*Sc olivine/melt to *D*MgO olivine/melt predicts *D*Sc = 0.32. Using the same equation and *D*MgO olivine/melt from our samples gives 0.32 to 0.37, which makes sense as *D*Sc should not change with fO_2 as it exists only as 3+.

Table 1 also shows decreasing *D*V olivine/melt with increasing fO_2. This is consistent with V^{3+} being more compatible in olivine than V^{4+} [7]. The reason for this may be due to the substitutional couple in which one vacancy can accomodate $2V^{3+}$ cations, while one vacancy can only accommodate one V^{4+} cation [1].

Table 2 presents Cr, Sc, and V wt. % oxide concentrations in pyroxene and melt for each charge. All the pyroxenes measured here are low-Ca pigeonites, with Wollastanite (Wo) values of approximately 5 to 8. *D*Cr pyroxene/melt generally increases with increasing fO_2 in our charges. Cr^{3+} is more compatible in pyroxene than Cr^{2+} so these results are valid. Our *D* values are also comparable to values determined by [8], which are *D*V = 3.5 at IW-1, 4.3 at IW, and 5.0 at IW+1. Our values show a large spread from charge to charge and more careful analyses are needed to rectify this.

Again, our *D*Sc values are not consistent at all (Table 2), and again this is most likely related to analytical error. The regression of [6], using *D*MgO pyroxene/melt, predicts *D*Sc = 1.3 for all charges. Using the same equation and *D*MgO pyroxene/melt from our charges yields comparable *D*s of 1.2 to 1.5.

Lastly, Table 2 shows that *D*V pyroxene/melt decreases with increasing fO_2. This is agreeable with the notion that DV^{3+} is more compatible in pyroxene than V^{4+}; which is probably because the charge balancing couple $^{M1}V^{3+}$ - ^{IV}Al is more compatible than in the pyroxene structure than $^{M1}V^{4+}$ - $2^{IV}Al$ owing to the charge balance couples [1] fO_2. Our *D*V values at each fO_2 are broadly consistent with those of [8], but the large variation in charges from the same fO_2 indicate we need more detailed and careful analyses.

Table 1. *D*Cr, *D*Sc and *D*V olivine/melt vs. fO_2.

IW-1		Cr			Sc			V		
T(°C)	Ol	gl	DCr	Ol	gl	DSc	Ol	gl	DV	Charge
1180	0.263	0.274	0.97	0.019	0.017	1.42	0.099	0.149	0.67	S15
1170	0.268	0.263	1.03	0.025	0.057	0.45	0.093	0.150	0.62	S16
1160	0.246	0.237	1.04	0.017	0.030	0.57	0.056	0.095	0.59	S17
1150	0.226	0.220	1.04	0.020	0.020	1.22	0.061	0.110	0.56	S18
1130	0.225	0.195	1.15	0.020	0.118	0.17	0.075	0.105	0.71	S7
	0.246	**0.238**	**1.04**	**0.020**	**0.048**	**0.76**	**0.077**	**0.122**	**0.63**	
IW										
1190	0.231	0.220	1.06	0.020	0.044	0.45	0.044	0.119	0.38	S9
1180	0.167	0.164	1.01	0.019	0.101	0.18	0.033	0.088	0.38	S10
1175	0.193	0.200	0.97	0.020	0.044	0.49	0.034	0.099	0.34	S13
1170	0.159	0.165	0.97	0.022	0.116	0.19	0.040	0.092	0.43	S11
1163	0.162	0.161	1.01	0.018	0.095	0.19	0.037	0.081	0.45	S12
1130	0.142	0.131	1.08	0.022	0.105	0.21	0.032	0.078	0.42	S8
	0.176	**0.173**	**1.02**	**0.020**	**0.084**	**0.28**	**0.037**	**0.093**	**0.40**	
IW+2										
1150	0.107	0.087	1.24	0.019	0.047	0.42	0.030	0.105	0.29	S20
	0.107	**0.087**	**1.24**	**0.019**	**0.047**	**0.42**	**0.030**	**0.105**	**0.29**	

Table 2. *D*Cr, *D*Sc and *D*V pyroxene/melt vs. fO_2.

IW-1		Cr			Sc			V		
T(°C)	pyx	gl	DCr	pyx	gl	DSc	pyx	gl	DV	Charge
1190	0.669	0.295	2.31	0.075	0.035	2.40	0.220	0.105	2.12	S14
1180	0.828	0.370	2.24	0.068	0.022	3.23	0.369	0.165	2.23	S15
1170	0.609	0.187	3.34	0.088	0.046	1.92	0.285	0.132	2.15	S16
1160	0.595	0.204	2.93	0.066	0.028	2.39	0.186	0.090	2.12	S17
1150	0.678	0.253	3.03	0.084	0.024	6.46	0.308	0.117	2.79	S18
1130	0.706	0.195	3.61	0.137	0.118	1.17	0.382	0.105	3.64	S7
1100	0.606	0.173	3.52	0.185	0.145	1.28	0.209	0.063	3.32	S6
	0.670	**0.240**	**3.00**	**0.100**	**0.060**	**2.69**	**0.280**	**0.111**	**2.63**	**AVG**
IW										
1170	0.459	0.165	2.79	0.090	0.116	0.77	0.169	0.090	1.87	S11
1163	0.685	0.161	4.26	0.126	0.095	1.32	0.257	0.081	3.17	S12
1130	0.667	0.131	5.11	0.121	0.105	1.16	0.243	0.078	3.11	S8
	0.604	**0.152**	**4.05**	**0.112**	**0.105**	**1.09**	**0.223**	**0.083**	**2.72**	**AVG**
IW+2										
1180	0.509	0.191	2.87	0.069	0.039	2.14	0.142	0.111	1.30	S21
1150	0.534	0.105	5.50	0.113	0.044	2.75	0.212	0.112	1.91	S20
	0.521	**0.148**	**4.18**	**0.091**	**0.042**	**2.44**	**0.177**	**0.111**	**1.61**	**AVG**

Acknowledgements: This work was supported by NASA grant NNX14AG30G to J.M. Karner.

References: [1] Papike, J.J., et al. (2005) *Am. Min., 90,* 277-290. [2] Kitts, K. and Lodders, K. (1998) *MAPS 33*, A197-A213. [3] Stolper, E.M. (1977) *GCA, 41,* 587-611. [4] Filiberto, J. and Dasgupta, R. (2011) *EPSL, 304,* 527-537. [5] Hanson, B.Z. and Jones, J.H. (1998) *Am. Min., 83,* 1151–1154. [6] Jones, J.H. (2016) *Geochem. Perspectives, 5-2,* 147-251. [7] Canil, D. and Fedortchouk, Y. (2001) *Can. Min. 39,* 319-330. [8] Karner, J.M. et al. (2007) *Am. Min. 92*, 1238-1241.